UNIVERSIDADE FEDERAL DO CEARÁ
CENTRO DE CIÊNCIAS
DEPARTAMENTO DE QUÍMICA ANALÍTICA E FÍSICO-QUÍMICA
PROGRAMA DE PÓS-GRADUAÇÃO EM QUÍMICA

GIZELE DO NASCIMENTO DE CASTRO

COMPUTATIONAL STUDY OF WATER ADSORPTION ON IRON SURFACES AND METALLIC ALLOYS

FORTALEZA
2025

GIZELE DO NASCIMENTO DE CASTRO

COMPUTATIONAL STUDY OF WATER ADSORPTION ON IRON SURFACES AND METALLIC ALLOYS

Dissertação apresentada ao Programa de Pós-Graduação em Química da Universidade Federal do Ceará, como requisito parcial à obtenção do título de mestre em Química. Área de concentração: Físico-química.

Orientador: Prof. Dr. Norberto de Kassio Vieira Monteiro.
Coorientadora: Prof. Dra. Adriana Nunes Correia.

FORTALEZA
2025

GIZELE DO NASCIMENTO DE CASTRO

COMPUTATIONAL STUDY OF WATER ADSORPTION ON IRON SURFACES AND METALLIC ALLOYS

Dissertação apresentada ao Programa de Pós-Graduação em Química da Universidade Federal do Ceará, como requisito parcial à obtenção do título de mestre em Química. Área de concentração: Físico-química.

Aprovada em: 31 / 07 / 2025.

BANCA EXAMINADORA

_____

Prof. Dr. Norberto de Kássio Vieira Monteiro (Orientador)
Universidade Federal do Ceará (UFC)

_____

Prof. Dr. Pedro de Lima Neto
Universidade Federal do Ceará (UFC)

_____

Prof. Dr. Ámison Rick Lopes da Silva
Universidade Federal do Vale do São Francisco (UNIVASF)

ACKNOWLEDMENTS

To my family, my parents, Pedro Souza de Castro and Maria Claudeni do Nascimento de Castro, and sister Geiciara do Nascimento de Castro, for all their support and encouragement, even though I do not understand what I do, but always rooting for my personal and professional growth.

To my love, Alisson Marley Rodrigues Alcantara, for holding my hand and reminding me daily how capable I am of achieving all my goals and making my dreams come true.

To my advisor, Norberto de Kássio Vieira Monteiro, and co-advisor, Adriana Nunes Correia, for believing in me and trusting me.

To the examining board for their availability and valuable suggestions.

To the members of GQT (Group of Theoretical Chemistry) for all their teachings and patience, especially Lucas Lima, for the conversations and advice, I will always remember Renato Veríssimo, Osmar Júnior, Marcus and Leonardo Paes with great affection.

To my friends, Rochele Sales, Magna Albuquerque, and Lucas Matos, who transformed difficult days into lighter ones and achievements into shared celebrations, my eternal gratitude for your support, your attentive listening, and your constant presence.

To Conselho Nacional de Desenvolvimento Científico e Tecnológico (CNPq), thank you for the financial support by maintaining the scholarship.

I am grateful to the Federal University of Ceará for the structure and opportunity to fulfill my dream of a master's degree.

Moreover, my sincere thanks to all those not mentioned but who participated directly or indirectly in this journey.

“Nothing in life is to be feared, it is only to be understood. Now is the time to understand more, so that we may fear less.”

Marie Curie

ABSTRACT

One solution to reduce the concentration of greenhouse gases (GHG) in the atmosphere is to replace fossil fuels with clean and renewable energy sources, such as green hydrogen. However, the method used, water electrolysis, is not yet widely used in the market due to its high cost, since this process uses electrocatalysts based on noble metals, scarce in nature, such as iridium and platinum. The present study uses a computational approach to investigate the water adsorption stage in iron, iron-cobalt and iron-nickel alloys; geometric optimization, molecular dynamics and electronic properties calculations were performed based on Density Functional Theory (DFT). The computational results show that the Gibbs energy of water adsorption is more spontaneous in the following order of symmetry cuts: (110) > (100) > (111). The addition of a nickel atom to the metal surface increased the partial density of states of the adjacent iron atoms, facilitating the adsorption of the water molecule, since it was in the position between the iron atom and the nickel atom that a greater availability of electronic states for the interaction was observed. In addition, the adsorption of the water molecule on the metal surface decreased the partial density of states of the iron atom. This behavior was observed for pure iron and metal alloys, when water interacts with the most favorable active site on the surface, indicating that the iron atom donates the density of states to the water molecule for adsorption.

Keywords: green hydrogen; iron alloys; adsorption; DFT.

RESUMO

Uma das alternativas para reduzir a concentração de gases de efeito estufa (GEE) na atmosfera consiste na substituição dos combustíveis fósseis por fontes de energia limpas e renováveis, como o hidrogênio verde. Entretanto, o método empregado para sua produção, a eletrólise da água, ainda não é amplamente utilizado no mercado devido ao seu elevado custo, uma vez que esse processo requer eletrocatalisadores baseados em metais nobres, escassos na natureza, como irídio e platina. O presente estudo adota uma abordagem computacional para investigar a etapa de adsorção da água em ligas de ferro, ferro-cobalto e ferro-níquel. Foram realizadas otimização geométrica, dinâmica molecular e cálculos de propriedades eletrônicas com base na Teoria do Funcional da Densidade (DFT). Os resultados computacionais indicam que a energia de Gibbs de adsorção da água é mais espontânea na seguinte ordem dos planos cristalográficos: (110) > (100) > (111). A adição de um átomo de níquel à superfície metálica aumentou a densidade parcial de estados dos átomos de ferro adjacentes, favorecendo a adsorção da molécula de água, uma vez que foi na posição entre o átomo de ferro e o átomo de níquel que se observou maior disponibilidade de estados eletrônicos para a interação. Adicionalmente, a adsorção da molécula de água na superfície metálica promoveu a diminuição da densidade parcial de estados do átomo de ferro. Esse comportamento foi observado tanto para o ferro puro quanto para as ligas metálicas, quando a água interage com o sítio ativo mais favorável na superfície, indicando que o átomo de ferro doa densidade de estados à molécula de água durante o processo de adsorção.

Palavras-chave: hidrogênio verde; ligas de ferro; adsorção; DFT.

SUMMARY

1 INTRODUCTION

Global warming represents one of today's environmental threats, driven mainly by the unbridled emission of greenhouse gases (GHG), mainly carbon dioxide (CO_2), resulting from the burning of fossil fuels (Singh; Banerjee; Hawkins, 2023). This imbalance has caused significant climate changes, severely impacting ecosystems, hydrological cycles and socioeconomic systems (Palermo et al., 2023). Given this scenario, developing and adopting sustainable and low-carbon energy technologies becomes urgent (Tang et al., 2023).

Green hydrogen emerges as a promising alternative to the traditional energy matrix in this context. Unlike gray or blue hydrogen, which is obtained from fossil sources, green hydrogen is produced via water electrolysis, an electrochemical process in which the H_2O molecule is dissociated into oxygen (O_2) and molecular hydrogen (H_2), using electrical energy from renewable sources, such as solar or wind (Saha et al., 2024). One of the products of water electrolysis is hydrogen gas, which can be used as a clean and renewable fuel due to its low greenhouse gas emissions into the atmosphere (Anwar et al., 2021). Considering that the product of burning hydrogen gas is water vapor, this becomes one of the main alternatives for replacing fossil fuels (Khan et al., 2018).

Electrolysis breaks down the water molecule, producing gaseous hydrogen and oxygen through reactions (Sebbahi et al., 2022).

Cathode: $2H_2O(l) + 2e^- \rightarrow H_2(g) + 2OH^-(aq)$ (1)

Anode: $2OH^-(aq) \rightarrow ½\ O_2(g) + H_2O(l) + 2e^-$ (2)

Global equation: $H_2O(l) \rightarrow H_2(g) + ½\ O_2(g)$ (3)

Electrolysis consists of an electrocatalytic decomposition, requiring a cathode and an anode responsible for the electrochemical semi-reactions. These electrodes are connected to an external energy source, thus forming a conductive circuit where electrons can be transferred (Zeng; Zhang, 2010). To break the water molecule and develop hydrogen gas, the water molecule first approaches the electrode at specific surface locations called active sites. The water molecule will be adsorbed at the site with the lowest energy barrier, which can favor the reaction; after the water molecule breaks, the hydrogens adsorbed on the surface can interact with each other or with the free water molecules within the solution to produce hydrogen (Alobaid; Wang; Adomaitis, 2018; Chang et al., 2023; Zeng et al., 2023).

Most of the electrocatalysts used for water electrolysis are based on noble metals, such as platinum, ruthenium, and iridium alloys (Wang, Lu; Zhong, 2021). However, these

metals are not abundant in the Earth's crust and become scarce and expensive (Wu et al., 2021). Large-scale implementation of this method of obtaining green hydrogen is unlikely due to the high cost and limited quantity of these elements available on the planet (Tüysüz, 2023). Therefore, studies on other materials, especially common transition metals, have grown due to their abundance and low cost. Ensuring the most economically competitive water electrolysis in the commercial use market (Huang et al., 2017).

Iron is an external transition metal with atomic number 26 and is the fourth most abundant element by mass in the Earth's crust (Cundy; Hopkinson; Whitby, 2008). This metal has always been present in the lives of living beings, whether in the manufacture of weapons and utensils or as part of their metabolism, making this element non-toxic to living beings and the environment. Therefore, iron is a good catalyst option (Casnati, Lanzi, Cera, 2020). Iron is a crystal whose main characteristic is the periodic repetition of atoms organized in space, that is, in three dimensions, giving the metal its shape (Hoffmann, 1987). This infinite and discrete arrangement, where the arrangement and orientation of the atoms are the same at any point in the lattice, is called the Bravais lattice. The continuation of the network is given by a unit cell, the smallest unit that allows the complete structure to be described through its repetition in space (Ashcroft; Mermin, 2005; Silva-Ramírez et al., 2023).

The unit cell for this metal is of the body-centered cubic (BCC) type; if the orientation of a plane of atoms in this unit cell is defined, we obtain the Miller indices (hkl), which are nothing more than an intersection of this plane with the axes of the cell's coordinate system, these indices are always defined in integers. This way, a symmetric plane can be passed through this cell and obtain different properties for a BCC unit cell. The plane that intersects the three axes at the vertices of the cell will have the indices (1 1 1), for example (Ladd, 2022). The other common indices for the iron unit cell are (1 1 0) and (1 0 0), considering the intercept at the cell vertex in each direction (Kwawu et al., 2017), as can be seen in Figure 1. Since it is a cubic cell, variations such as (1 0 0), (0 1 0) and (0 0 1) of the Miller index are equivalent to each other; it is not necessary to study all of them, with only one being chosen to represent the others (Błoński; Kiejna, 2007).

The study of surfaces with different Miller indices is important because it determines the stability of the material (Blakely; Somorjai, 1977; Huang, Luo, Yao, 2010). In other words, for the analyzed metal to be considered an efficient catalyst, in addition to reducing the activation energy and increasing the speed of a reaction, it also needs to resist the conditions in which the reaction is occurring since one of the characteristics of a catalyst is to be inert, that is, it is not reactive and is not consumed in the process, making it possible to

obtain it practically unchanged at the end of the reaction (Grünert; Kleist; Muhler, 2023). It is known, however, that iron is quite reactive and quickly oxidizes in contact with water, losing its metallic characteristics. However, when combined with other metals, it can produce corrosion-resistant alloys, especially those that contain nickel and cobalt in their composition.

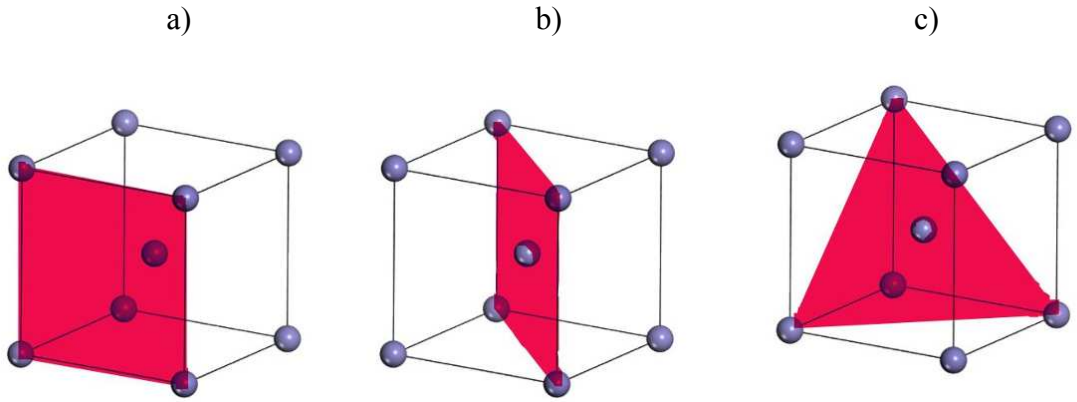

Figure 1: Representation of the Miller index of the iron unit cell in a) (1 0 0), b) (1 1 0) and c) (1 1 1).

Testing new materials can become arduous, considering the costs and time involved in synthesizing the material and conducting several experiments to test the properties. Therefore, theoretical calculations to analyze these materials with computational simulations become extremely necessary and viable (Skogh et al., 2023). Therefore, the work aims to present the water adsorption stage on iron surfaces and their subsequent metal alloys with cobalt and nickel. The work was carried out theoretically using the Cambridge Serial Total Package (CASTEP) software, which is based on Density Functional Theory (DFT) and is responsible for computational simulations of metal supercells. Geometric optimization calculations were performed to determine these materials' adsorption energy and electronic properties to decide the best alternative to replace noble metals in electrocatalysts.

2 COMPUTATIONAL STUDY OF WATER ADSORPTION ON IRON SURFACES AND METALLIC ALLOYS

Abstract

One solution to reduce the concentration of greenhouse gases (GHG) in the atmosphere is to replace fossil fuels with clean and renewable energy sources, such as green hydrogen. However, the method used, water electrolysis, is not yet widely used in the market due to its high cost, since this process uses electrocatalysts based on noble metals, scarce in nature, such as iridium and platinum. The present study uses a computational approach to investigate the water adsorption stage in iron, iron-cobalt and iron-nickel alloys; geometric optimization, molecular dynamics and electronic properties calculations were performed based on Density Functional Theory (DFT). The computational results show that the Gibbs energy of water adsorption is more spontaneous in the following order of symmetry cuts: (110) > (100) > (111). The addition of a nickel atom to the metal surface increased the partial density of states of the adjacent iron atoms, facilitating the adsorption of the water molecule, since it was in the position between the iron atom and the nickel atom that a greater availability of electronic states for the interaction was observed. In addition, the adsorption of the water molecule on the metal surface decreased the partial density of states of the iron atom. This behavior was observed for pure iron and metal alloys, when water interacts with the most favorable active site on the surface, indicating that the iron atom donates the density of states to the water molecule for adsorption.

Keywords: green hydrogen; iron alloys; adsorption; DFT.

1. Introduction

It is estimated that 2030 energy demand will increase by up to 50%, according to the International Energy Agency (IEA)[1], because the world's population is growing rapidly, and the search for energy is becoming increasingly necessary[2]. However, it is known that since the Industrial Revolution, the most used energy source worldwide has been fossil fuels, such as oil and natural gas[3]. Although it is responsible for 95% of energy supply, fossil fuel specifically has, among others, an increased concentration of gases such as carbon dioxide (CO_2) and methane (CH_4) in the atmosphere, which contributes to global warming. The increase in the planet's temperature causes climate change accompanied by environmental disasters.

Therefore, in 1997, the Kyoto Protocol was adopted to considerably reduce the

emission of greenhouse gases (GHG)[4] into the atmosphere. Furthermore, the amount of this raw material on the planet is limited and is rapidly depleting, which makes fossil fuels non-renewable energy sources. Therefore, searching for renewable energy sources with low or no GHG emissions is essential, and Green hydrogen stands out among the alternatives[5].

To be considered green, hydrogen gas must be produced using methods considered green, and for this, the process must be free of GHG emissions. However, around 95% of this gas produced worldwide comes from non-renewable sources, such as natural gas[6]. Under these circumstances, a clean and effective way to produce hydrogen gas is through the electrolysis of water[7] with electrical energy responsible for initiating the electrochemical reactions of the process, coming from renewable and clean sources such as wind and solar energy [8,9].

Electrolysis consists of an electrocatalytic decomposition, requiring a cathode and an anode responsible for the electrochemical half-reactions. These electrodes are connected to an external energy source, thus forming a conductive circuit where electrons can be transferred[10]. To break the water molecule and develop hydrogen gas, the water molecule first approaches the electrode in specific locations on the surface. The water molecule will be adsorbed in the site with the lowest energy barrier, which can favor the reaction. Some mechanisms, widely studied and available in the literature, occur on the catalyst surface, such as the Volmer, Heyrovsky and Tafel steps, until the final product of interest, H_2, is produced to be desorbed[11–13].

However, the production of green hydrogen using water electrolysis is not the smallest percentage of global production by chance, being only approximately 5%[14]. This is mainly due to economic reasons, which are quite expensive and unfeasible due to using renewable energy in these processes, which involves some challenges, such as the location for installation and maintenance[15,16] as well as the materials used during the process[17,18]. For this reason, research has been carried out in search of new materials and technologies to optimize and make this method economically viable, one of which is the replacement of noble metals, such as platinum, in electrocatalysts with materials that are more abundant in the Earth's crust[19].

A good catalyst speeds up electrochemical reactions; that is, it will reduce the activation energy required to initiate the half-reactions that begin with the adsorption of the water molecule onto the catalyst[20]. One of the indispensable characteristics of a good electrocatalyst is that it is resistant and stable to electrochemical degradation in high currents 4 densities. Furthermore, the material must be low-cost and abundant to be widely used

implemented in the market[21]. Most electrocatalysts used for water electrolysis are based on noble metals, such as platinum, ruthenium and iridium alloys[22]. However, these metals have low abundance in the Earth's crust and consequently become scarce and expensive[23]. Large-scale implementation of this method of obtaining green hydrogen is unlikely due to the high cost and limited quantity of these elements available on the planet[24].

Therefore, studies with other materials, especially common transition metals, have grown due to their abundance and low cost. This is essential to ensure the most economically competitive water electrolysis in the commercial use market [25]. Iron is an external transition metal with atomic number 26 and is the fourth most abundant element by mass in the Earth's crust [26]. This metal has always been present in the lives of living beings, whether for the manufacture of weapons and utensils or as part of their metabolism, making this element non-toxic to living beings and the environment. Therefore, iron stands out as a good option for a catalyst [27]. Thus, it is interesting to analyze iron and some of its metal alloys, such as cobalt and nickel, as an alternative to replace noble metals in electrocatalysts. Fe-Co and Fe-Ni alloys are widely studied and mentioned in the literature [28–30], so analyzing these materials in water electrolysis is also necessary.

To test new materials, arduous research and experiments are necessary to synthesize and determine properties and characteristics, which requires much time and financial investment. However, an effective way is to use theoretical calculations to analyze interactions and predict some information about these[31]. In adsorption, one of the advantages of using computational calculations is to reduce the time and cost of research to analyze new catalysts, with the freedom of being able to work with any material without necessarily having it physically[32]. In this way, through computational calculations, it is possible to predict some properties and the ability to simulate specific temperature and pressure conditions. Verifying adsorption energy, spontaneity and kinetics, in addition to the behavior of the adsorbate on the surface through simulations, thus being an indispensable tool for advancing scientific knowledge and saving resources[33].

Therefore, the work aims to present the first stage of water adsorption on iron surfaces and their subsequent metal alloys with cobalt and nickel. The work was carried out based on the Density Functional Theory (DFT) and is responsible for computational simulations of metallic supercells. Geometric optimization calculations were carried out to determine the Gibbs energy of adsorption and electronic properties of these materials to decide the best alternative to replace noble metals in electrocatalysts, make water electrolysis cheaper and expand as the main method of producing green hydrogen.

2. Computational details

The calculations were performed using the Cambridge Serial Total Energy Package (CASTEP)[34,35]. This software, based on Density Functional Theory (DFT)[36–38], is a widely accepted quantum mechanics code for simulating surfaces of crystalline and amorphous solids. The functional used was the Generalized Gradient Approximation (GGA) parameterized by Perdew-Burke-Ernzerhof (PBE)[39] with a cutoff energy of 581 eV was employed. A $3 \times 3 \times 1$ Monkhorst-Pack grid was defined for k-point sampling of the Brillouin Zone (BZ)[40] For the geometric optimization calculations, the Broyden-Fletcher-Goldfarb-Shanno (BFGS)[41–43] algorithm was used, with convergence tolerances defined as a maximum force of 0.03 eV/Å, maximum energy change of 10^{-5} eV/atom, maximum displacement of 0.001 Å, and maximum stress of 0.5 GPa[44] for all analyzed systems.

The first step was to perform the geometric optimization of a pure iron unit cell; from this, three supercells were constructed with three different symmetry cuts corresponding to the Miller indices (1 0 0), (1 1 0), and (1 1 1), Each supercell represents, at the microscopic level, the events occurring throughout the catalyst. Due to periodic boundary conditions, it can be assumed that this system represents the entire length of the electrocatalyst[45]. Furthermore, the supercells were constructed with a 12 Å vacuum, primarily to prevent interactions between the top layer and the underlying layer, and to accommodate the water molecule.

Subsequently, the supercells were geometrically optimized to allow proper relaxation of the surface iron atoms. Since adsorption is a surface phenomenon [46], the Cartesian coordinates of the iron atoms the innermost layerx of the surface were fixed to minimize computational cost. After the supercells were completed, a water molecule was constructed and geometrically optimized. The water molecule was then randomly added approximately 1.5 Å above the pure iron surface, forming an Fe-water system.

The next step involved the construction of three new supercells with the same Miller indices, (1 0 0), (1 1 0) and (1 1 1), but one iron atom in each of the three supercells was replaced by a cobalt atom to simulate a Fe-Co metallic alloy. This same methodology was used to construct the three surfaces of the Fe-Ni alloy. In total, nine systems were constructed: three for pure iron, three for the Fe-Co metal alloy and three for the Fe-Ni metal alloy, and three different Miller indices (1 0 0), (1 1 0) and (1 1 1) were analyzed for each material, In Fig. 1, it is possible to verify the three systems assembled for the Miller index (1 0 0). Once the surfaces were finished, molecular dynamics were performed on each of the systems, using

the NVT ensemble, with the temperature set at 298 K, using the Nose-Hoover thermostat[47].

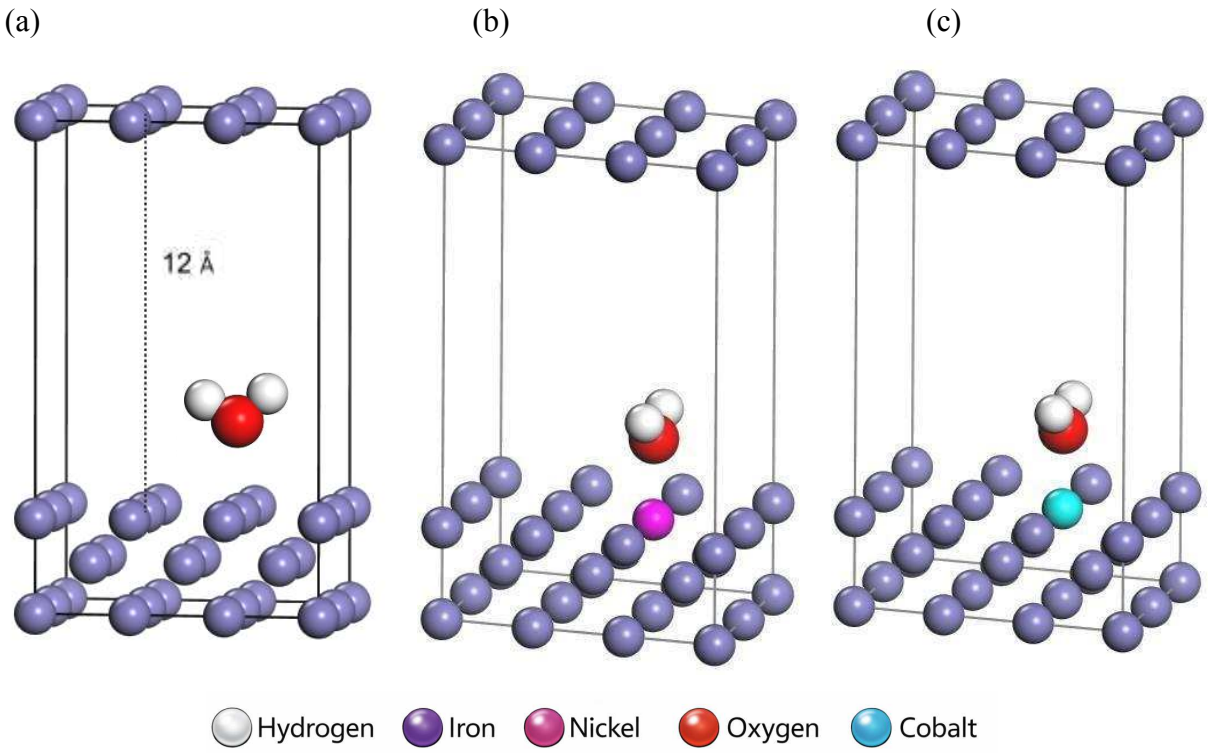

Fig. 1. Systems formed by the water molecule on a a) Fe(1 0 0) surface, b) Fe (1 0 0)-Ni alloy and c) Fe(1 0 0)-Co alloy.

At the end of the dynamics, the frame with the lowest energy adsorbent-adsorbate position for each system was isolated and geometrically optimized to determine the most favorable active site. Subsequently, optimizations were performed for the surface without the adsorbate and for the adsorbate without the surface to determine the system's adsorption energy. The values obtained were added to a table 1, and the Gibbs adsorption energy ($\Delta G_{adsorption}$) for each system was determined using equation (1), which relates the G values for the adsorbate-adsorbent system and the individual energies of each one.

The Gibbs energy of adsorption can be calculated by equation (1), where ($\Delta G_{adsorption}$) is the change in Gibbs energy for adsorption, (G_{system}) is the energy of the water-metal system, ($G_{surface}$) is the energy of the metal surface only, and ($G_{adsorbate}$) is the energy for the water molecule only. After determining the $\Delta G_{adsorption}$ values, calculations were performed to determine electronic properties such as Partial Density of States (PDOS) and Total Density of States (TDOS) before and after adsorption for comparison.

$$\Delta G_{adsorption} = G_{system} - (G_{surface} + G_{adsorbate}) \quad (1)$$

Furthermore, weak forces involved in the system, such a Independent Gradient Model (IGM), were analyzed, the results were treated using the Multiwfn[48] software 3.8, and images were rendered using Visual Molecular Dynamics (VMD)[49] software.

3. Results and discussion

3.1 Determining the Gibbs Energy for the Systems

Molecular dynamics was used to locate the lowest-energy site on the electrocatalyst surface. During the simulation, the water molecule was free to interact with the surface and adsorb at the most favorable position. The values of $\Delta G_{adsorption}$ for each system are presented in Table 1.

Table 1. Values of Energy Gibbs of all systems analyzed in kcal mol^{-1}

Miller index	Surface	ΔG_{system} / kcal mol^{-1}	$\Delta G_{surface}$ / kcal mol^{-1}	$\Delta G_{adsorbato}$ / kcal mol^{-1}	$\Delta G_{adsorption}$ / kcal mol^{-1}
(1 0 0)	Fe	-368534.73	-357658.86	-10867.22	-8.63
	Fe-Co	-373990.47	-363121.70	-10867.17	-1.59
	Fe-Ni	-380068.87	-369191.60	-10867.61	-9.65
(1 1 0)	Fe	-249319.51	-238442.29	-10868.05	-9.15
	Fe-Co	-254780.90	-243910.93	-10868.17	-1.79
	Fe-Ni	-260853.81	-249976.63	-10867.36	-9.82
(1 1 1)	Fe	-368258.19	-357388.61	-10867.62	-1.96
	Fe-Co	-373723.71	-362855.09	-10867.65	-0.95
	Fe-Ni	-379793.99	-368924.23	-10867.26	-2.49

The table 1 shows that all systems adsorption process occurred spontaneously due to the negative values for $\Delta G_{adsorption}$ [50]. However, it is observed that the systems with pure iron and Fe-Ni alloys are more spontaneous, especially with the Fe-Ni alloy, as they present the lowest $\Delta G_{adsorption}$ values, compared to the Fe-Co alloy. This does not necessarily imply a more pronounced catalytic characteristic. The theoretical values obtained align with experimental studies that demonstrated the good performance of binary metal alloys based on iron, cobalt[51] and nickel[52], specifically, as electrocatalysts for water electrolysis in hydrogen production.

The position in which the water molecule approaches the surface of the electrocatalyst is always with the oxygen atom facing the surface starting the Volmer stage; upon receiving an electron, a hydrogen atom is adsorbed on the electrocatalyst, releasing a hydroxyl into the medium. Analyzing only pure iron, it is clear that the water molecule approaches the surface between two iron atoms for all Miller indices.

In the Miller indices (1 0 0) and (1 1 1), in both Fe-Co and Fe-Ni, the water molecule approaches between an iron atom and a cobalt atom in the Fe-Co alloy and between an iron atom and a nickel atom in the Fe-Ni alloy. In the Miller index (1 1 0), the water molecule approached the surface of the metallic alloys just above the iron atom close to the cobalt atom in the Fe-Co alloy and the iron atom close to the nickel in the Fe-Ni alloy.

3.2 Analyzing Adsorption Energies and Stability of Symmetry Cuts

Based on the results in Table 1, information about the stability of the studied symmetry cuts can be inferred. For the Miller index (1 0 0), it was observed that adding a cobalt atom to the iron surface significantly disfavored the adsorption of the water molecule, changing $\Delta G_{adsorption}$ from −8.63 kcal mol^{-1} to −1.59 kcal mol^{-1}. Conversely, the addition of a nickel atom favored the adsorption process, decreasing the energy from −8.63 kcal mol^{-1} to −9.65 kcal mol^{-1}.

The (1 1 0) index followed a similar trend: energy increased with cobalt addition, from −9.15 kcal mol^{-1} to −1.79 kcal mol^{-1}, and decreased with nickel addition, from −9.15 kcal mol^{-1} to −9.82 kcal mol^{-1}. For surfaces with index (1 1 1), the most positive $\Delta G_{adsorption}$ values were obtained, but nickel addition still favored water adsorption, changing the energy from −1.96 kcal mol^{-1} to −2.49 kcal mol^{-1}, while cobalt addition disfavored it compared to pure iron, increasing the adsorption energy from −1.9617 kcal/mol to −0.95 kcal mol^{-1}.

Thus, for all symmetry cuts, cobalt addition increases the adsorption energy

and consequently disfavors adsorption, whereas nickel addition decreases the energy, favoring water molecule adsorption in these systems compared to pure iron. This is a satisfactory result considering that nickel is cheaper and less toxic than cobalt[53]. Therefore, using nickel metallic alloys as stable and energetically favorable electrocatalysts for water adsorption becomes viable both thermodynamically and economically. Experimental studies have shown the effectiveness of nickel-based electrocatalysts, whether alloyed with iron or even oxides, surpassing elements like iridium, a noble metal also used for water electrolysis[54].

A greater stability in systems with symmetry cuts (1 0 0) and (1 1 0) can also be observed, especially for the (1 1 0) symmetry cut. When comparing $\Delta G_{adsorption}$ values for pure iron, the indices rank from most to least stable as (1 1 0) < (1 0 0) < (1 1 1), and the same sequence applies to the metallic alloys. Among the three Miller indices, (1 1 0) yielded the most favorable values, making it the most stable of the three. This stability trend can be explained by the greater atomic packing in the supercells. As shown in Fig. 2, the Miller index (1 1 0) has tighter atomic packing due to the proximity of the atoms, reducing the surface energy and consequently making it more stable compared to the other indices[55].

(a)

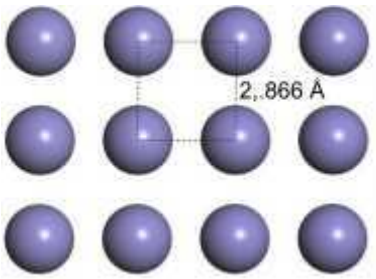

(1 0 0)

(b)

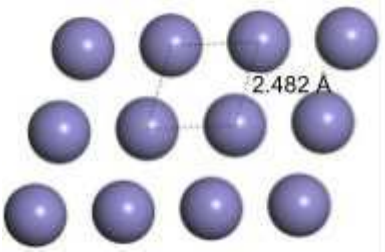

(1 1 0)

(c)

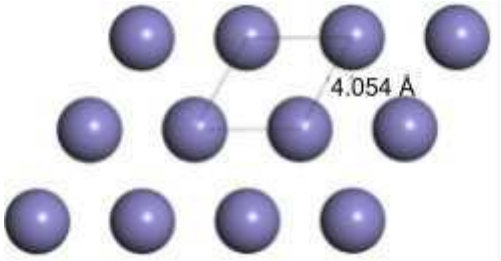

(1 1 1)

Fig. 2. The iron surfaces and their respective distance between atoms with Miller indices

3.3 Density of States

The Density of States (DOS) was calculated for all analyzed systems. This electronic property quantitatively indicates the number of electronic states available per unit of energy for electrons to occupy[56]. Partial Density of States (PDOS) allows examination of the electronic states available per orbital of a specific atom. At the same time, the Total Density of States shows all electronic states without differentiating orbitals. The TDOS of the systems can be verified in Fig.S3, S4 and S5 in the supplementary material.

This work calculated the PDOS for a single iron atom that directly interacted with the water molecule. This analysis was carried out to understand the behavior of the electronic states of the iron atom in each system before and after the addition of cobalt and nickel atoms to the surface, as well as before and after the adsorption of the water molecule. Fig. 3a, 3b and 3c showed the PDOS for the Fe surface, Fe-Co alloy and Fe-Ni alloy, respectively.

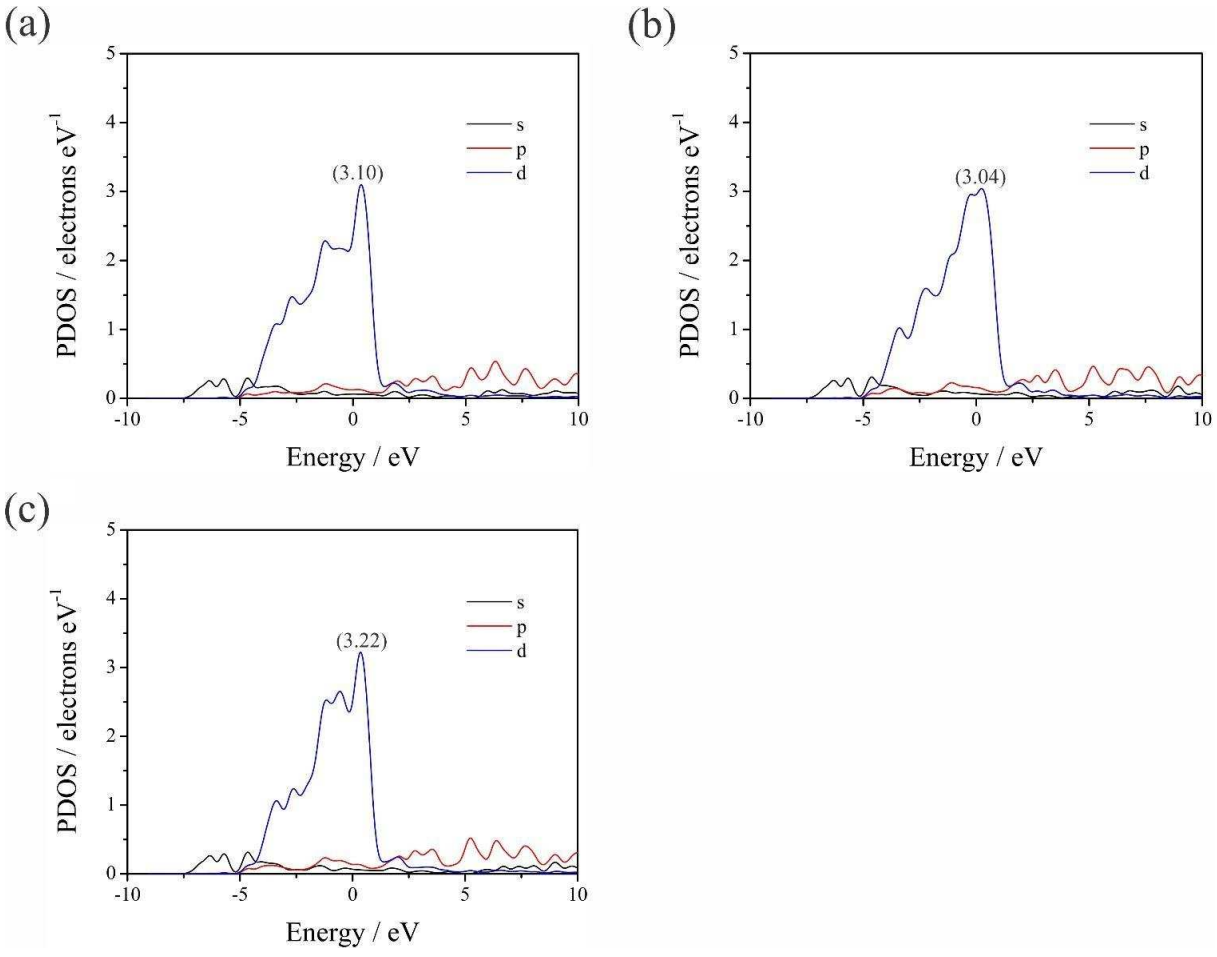

Fig. 3. PDOS for a) Fe surface, b) Fe-Co alloy and c) Fe-Ni alloy.

It is immediately apparent that, on all surfaces, the d orbital of the iron atom shows the largest peaks in the Fig.3, representing the level with the greatest number of electronic states available for interaction with water molecule. According to Fig. 3a, the highest number of available states for pure iron in the d orbital is in the largest peaks, the first 3.10 electrons eV^{-1}, which is in the conduction band. In Fig. 3b, the addition of cobalt descreased the density of the state of iron to 3.04 electrons eV^{-1}, and nickel increased it to 3.22 electrons eV^{-1}, as shown in Fig. 3c. It explains why a water molecule approaches the surface near the iron atoms and not the nickel or cobalt atoms, since the nickel atoms increase the availability of the iron atom's orbitals to interact with the water molecule. Even though adding cobalt to the surface decreased the density of states of the nearby iron atom, it was not significant enough that there was no interaction with the water molecule. However, it can be seen that in comparison, the addition of the nickel atom favors adsorption because it increases the number of available states.

The PDOS for cobalt and nickel atoms on surfaces with Miller index (1 1 0) can be seen in Fig. 4. It is noted that the electronic states available for interaction in the cobalt atom are smaller than that of iron, being 2.91 electrons eV^{-1}. However, the nickel atom has a higher state density than iron, 3.73 electrons eV^{-1}. Moreover, this explains why the water molecule does not adsorb between the iron atom and the cobalt or nickel atom. It can also be observed that the addition of nickel increased the electron density of the d orbital of the iron atom more than the addition of cobalt, which explains the more favorable values for the Fe-Ni metallic alloy

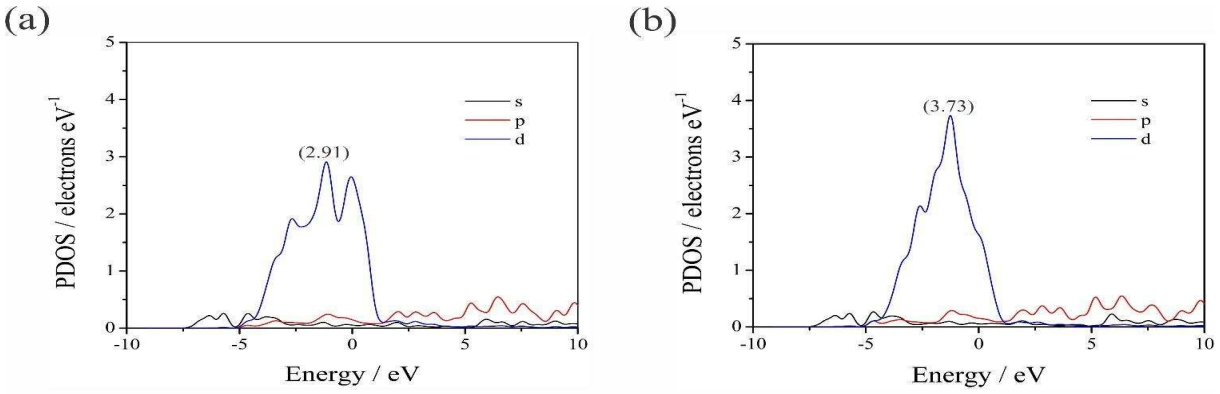

Fig. 4. PDOS for a) cobalt atom and b) nickel atom.

The Fig. 5 show the PDOS for the systems after the adsorption of the water molecule. In all systems, before and after adsorption, the d orbital of the iron atom has the greatest interaction availability, represented by the largest peaks. However, it is clear that the addition of the water molecule to the surface of Fe and the Fe-Ni alloy decreased the density of iron states much more, while in the Fe-Co alloy, the density of iron states increased. Furthermore, it can be seen that the d orbital peak is close to the Fermi level, in the conduction band, enabling electron transfer [57].

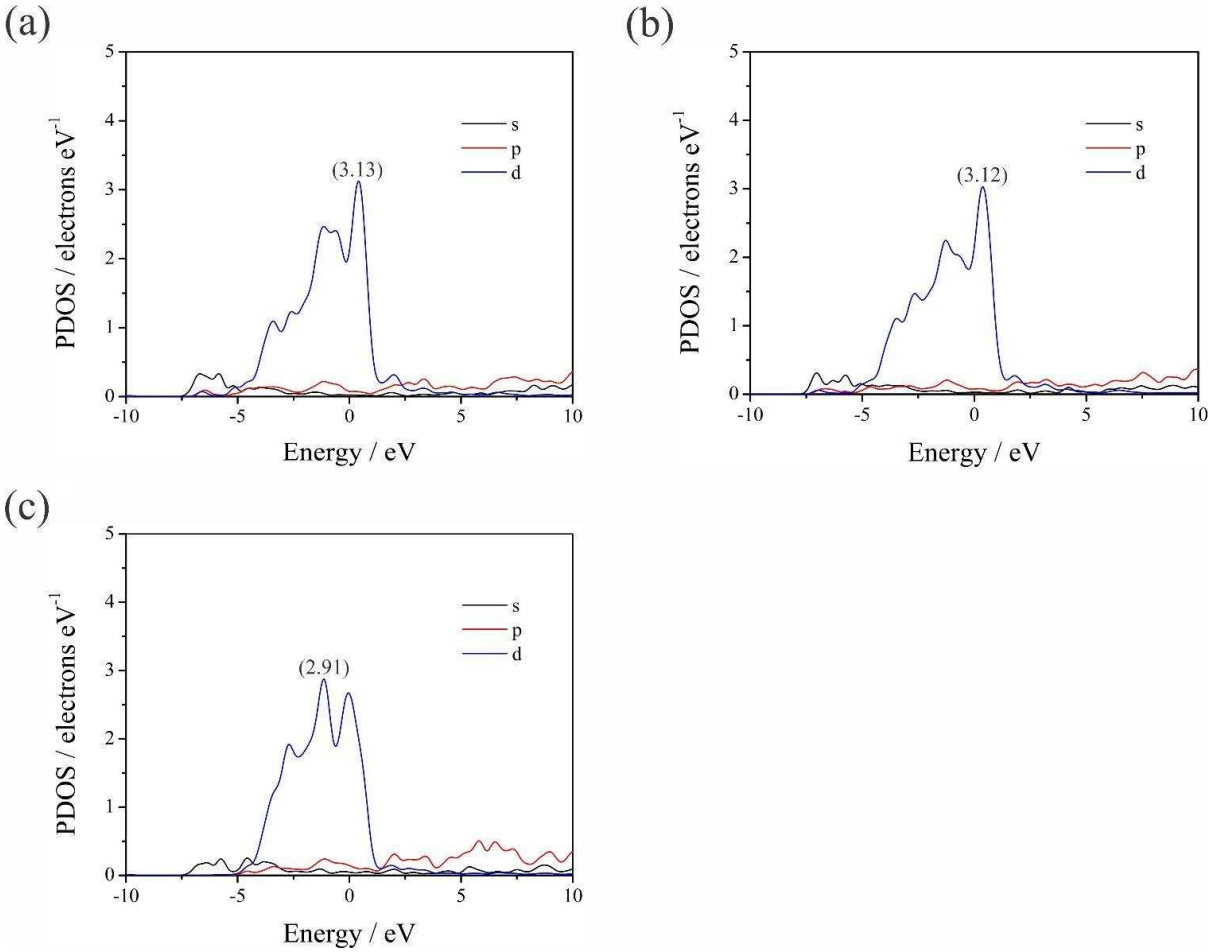

Fig. 5. PDOS for a) Fe-Co, b) Fe-Ni alloy and c) Fe, surfaces with water.

The water molecule is preferentially adsorbed with the oxygen atom pointing towards the surface in all systems. The diagram based on the Molecular Orbital Theory shows that the water molecule has empty antibonding orbitals[58]. Therefore, this tendency can be explained by iron donating electronic density to water, which occupies the antibonding orbitals, making the molecule unstable and facilitating the breaking of the O – H bond. However, the iron atom has electronic states available in the valence and conduction bands,

mainly in the d orbital. Thus, in addition to donating the density of states, iron also receives it, facilitating interaction and adsorption.

The following results show the isosurfaces for the interaction between the water molecule and the surfaces for the Miller index (1 1 0). In Fig. 6, it is possible to verify the isosurfaces of the IGM isosurface of the systems, the colors in the figures indicate how strong this interaction is occurring. Red indicates repulsive forces, while green indicates weak interactions, such as Van der Waals forces, and blue indicates stronger interactions, such as hydrogen bonds, for example. Analyzing the interactions in these systems, it is clear that the interactions between the isosurfaces of pure iron and the Fe-Ni alloy with the water molecule are much greater, indicated by the intense blue in systems 6a and 6b, while on the Fe-Co surface, 6c, there is a reddish coloration between the water molecule and the surface indicating a repulsion[59], which indicates a disfavoring of adsorption, implying more positive values of Gibbs energy that were verified in Table 1.

(a) Fe

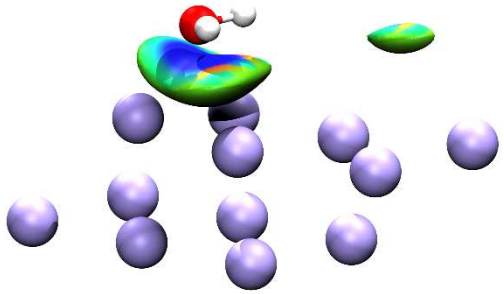

(b) Fe-Ni

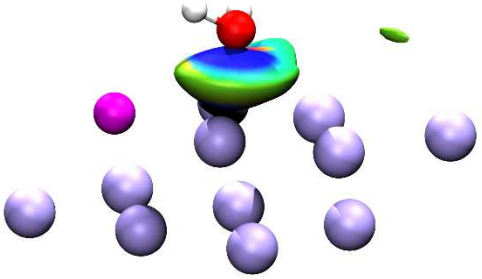

(c) Fe-Co

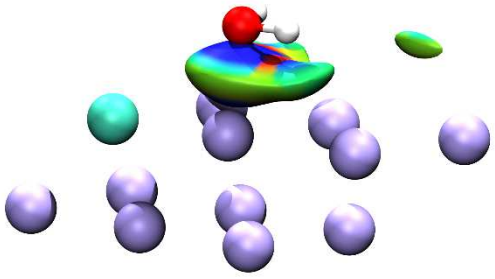

Fig. 6. The IGM isosurface of the systems a) Pure iron, b) iron alloy with nickel and c) iron alloy with cobalt, all analyzed for the Miller index (1 1 0).

In Fig. 7 below, it is possible to observe the IGM for pure Iron 7a and the Fe-Ni alloy 7b; which also serves to verify the interaction between the metal surface and the water

molecule during adsorption. The positive sign values in Fig. 7 show interactions of a repulsive nature, while the negative values represent attractive interactions, so it can be concluded that the more shifted to the left, the greater the attractive interactions for the system[60]. Fig. 7 shows that the adsorption in the Fe-Ni alloy shifted the peak in pure Iron to more negative values, indicating stronger interactions, which can explain the more negative values of the Gibbs Energy for the Fe-Ni system, thus explaining the more negative values and, consequently, more favorable for the Fe-Ni alloy compared to pure iron in Table 1.

(a) Fe

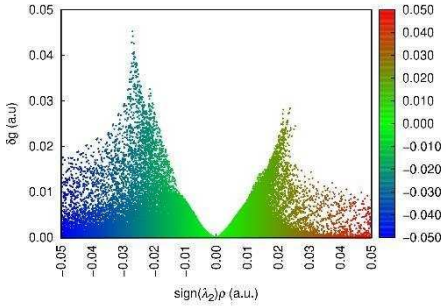

(b) Fe-Ni

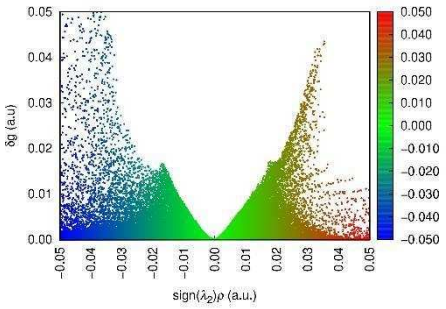

Fig. 7. The δg vs sign(λ_2)ρ for the interactions during the absorption of the water molecule in a) pure iron and b) iron and nickel alloy.

4 Conclusion

Simulations performed using DFT determined the Gibbs energy of adsorption and density of states for all analyzed systems. This analysis revealed that the most stable symmetry cut for working with iron and its metallic alloys is (1 1 0), followed by (1 0 0). The stability of the symmetry cuts is directly related to the surface size, i.e., the spatial arrangement of atoms in the crystal lattice, which reduces lateral repulsions and favors adsorbate adsorption at active sites. During the adsorption study, it was observed that the water molecule approaches the surface preferentially with the oxygen atom pointing toward it, due to the donation and acceptance of electronic states between iron and the adsorbate's oxygen. It was also determined that the lowest-energy site for water adsorption can vary with the Miller index. From the PDOS for the (1 1 0) symmetry cut, the addition of cobalt and nickel increased the density of states of the iron atom on the surface. This demonstrates that interaction with the adsorbate occurs preferentially at iron atoms because they have a higher density of states available for interaction. A consistent trend was observed wherein the partial density of states of iron always decreases with water adsorption across all Miller indices. This occurs due to the antibonding orbitals in the water molecule, causing iron to donate density of states during adsorption. Based on all the data obtained in this work, it can be concluded that the first adsorption step, for the water molecule on pure iron surfaces and their Fe-Co and Fe-Ni alloys occurs spontaneously, given the negative values of Gibbs energy of adsorption. However, the focus of this study was to analyze the adsorption of water in the materials investigated, and it can be concluded that the methodology employed successfully enabled the verification of the adsorption stage in the iron alloys.

ORCID

Gizele do Nascimento de Castro: https://orcid.org/0009-0008-1082-7729
Leonardo Paes da Silva: https://orcid.org/0000-0002-9264-4721
Lucas Lima Bezerra: http://orcid.org/0000-0002-6871-3045
Adriana Nunes Correia: https://orcid.org/0000-0002-3357-0160
Pedro de Lima Neto: https://orcid.org/0000-0002-1613-4797
Norberto de Kássio Vieira Monteiro: http://orcid.org/0000-0002-5847-5733

Author contributions

Gizele do Nascimento de Castro: investigation, methodology, validation, formal analysis, writing – original draft. Lucas Lima Bezerra: reviewing & editing. Leonardo Paes da

Silva: formal analysis, reviewing & editing. Adriana Nunes Correia: reviewing & editing. Pedro de Lima Neto: resources, writing – reviewing & editing. Norberto de Kássio Vieira Monteiro:resources, supervision, writing –reviewing & editing.

Declaration of competing interest

The authors declare that they have no known competing financial interests or personal relationships that could have appeared to influence the work reported in this paper.

Acknowledgments

The authors thank the Conselho Nacional de Desenvolvimento Científico e Tecnológico (CNPq) for its financial support and the Centro Nacional de Processamento de Alto Desempenho (CENAPAD) of the Universidade Federal do Ceará (UFC) and Centro Nacional de Processamento de Alto Desempenho em São Paulo (CENAPAD-SP) for the computational resources it offered.

References

[1] IEA, Renewables 2019 – Analysis - IEA, International Energy Agency (2019).
[2] S. Shiva Kumar, H. Lim, An overview of water electrolysis technologies for green hydrogen production, Energy Reports 8 (2022). https://doi.org/10.1016/j.egyr.2022.10.127.
[3] E.A. Wrigley, Energy and the english industrial revolution, Philosophical Transactions of the Royal Society A: Mathematical, Physical and Engineering Sciences 371 (2013). https://doi.org/10.1098/rsta.2011.0568.
[4] A. Mikhaylov, N. Moiseev, K. Aleshin, T. Burkhardt, Global climate change and greenhouse effect, Entrepreneurship and Sustainability Issues 7 (2020). https://doi.org/10.9770/jesi.2020.7.4(21).
[5] C. Tarhan, M.A. Çil, A study on hydrogen, the clean energy of the future: Hydrogen storage methods, J Energy Storage 40 (2021). https://doi.org/10.1016/j.est.2021.102676.
[6] H.H. Cho, V. Strezov, T.J. Evans, A review on global warming potential, challenges and opportunities of renewable hydrogen production technologies, Sustainable Materials and Technologies 35 (2023). https://doi.org/10.1016/j.susmat.2023.e00567.
[7] N.H. Alotaibi, S. Manzoor, S. Saleem, S. Mohammad, M. Khalil, Ş. Yalçin, A.G. Abid, S.I. Allakhverdiev, Rational development of PPy/CuWO4 nanostructure as competent electrocatalyst for oxygen evolution, and hydrogen evolution reactions, Int J Hydrogen Energy 59 (2024). https://doi.org/10.1016/j.ijhydene.2024.02.125.
[8] Q. Hassan, A.Z. Sameen, H.M. Salman, M. Jaszczur, Large-scale green hydrogen production via alkaline water electrolysis using solar and wind energy, Int J Hydrogen Energy 48 (2023). https://doi.org/10.1016/j.ijhydene.2023.05.126.
[9] M. Benghanem, A. Mellit, H. Almohamadi, S. Haddad, N. Chettibi, A.M. Alanazi, D. Dasalla, A. Alzahrani, Hydrogen Production Methods Based on Solar and Wind Energy: A Review, Energies (Basel) 16 (2023). https://doi.org/10.3390/en16020757.
[10] K. Zeng, D. Zhang, Recent progress in alkaline water electrolysis for hydrogen production and applications, Prog Energy Combust Sci 36 (2010).

https://doi.org/10.1016/j.pecs.2009.11.002.
[11] T.B. Ferriday, P.H. Middleton, M.L. Kolhe, Review of the hydrogen evolution reaction—a basic approach, Energies (Basel) 14 (2021). https://doi.org/10.3390/en14248535.
[12] X.Y. Zhang, J.Y. Xie, Y. Ma, B. Dong, C.G. Liu, Y.M. Chai, An overview of the active sites in transition metal electrocatalysts and their practical activity for hydrogen evolution reaction, Chemical Engineering Journal 430 (2022). https://doi.org/10.1016/j.cej.2021.132312.
[13] T. Schuler, T. Kimura, T.J. Schmidt, F.N. Büchi, Towards a generic understanding of oxygen evolution reaction kinetics in polymer electrolyte water electrolysis, Energy Environ Sci 13 (2020). https://doi.org/10.1039/d0ee00673d.
[14] F. Yu, L. Yu, I.K. Mishra, Y. Yu, Z.F. Ren, H.Q. Zhou, Recent developments in earth-abundant and non-noble electrocatalysts for water electrolysis, Materials Today Physics 7 (2018). https://doi.org/10.1016/j.mtphys.2018.11.007.
[15] S. Ramakrishnan, M. Delpisheh, C. Convery, D. Niblett, M. Vinothkannan, M. Mamlouk, Offshore green hydrogen production from wind energy: Critical review and perspective, Renewable and Sustainable Energy Reviews 195 (2024). https://doi.org/10.1016/j.rser.2024.114320.
[16] A.Z. Arsad, M.A. Hannan, A.Q. Al-Shetwi, R.A. Begum, M.J. Hossain, P.J. Ker, T.I. Mahlia, Hydrogen electrolyser technologies and their modelling for sustainable energy production: A comprehensive review and suggestions, Int J Hydrogen Energy 48 (2023). https://doi.org/10.1016/j.ijhydene.2023.04.014.
[17] D. Agrawal, N. Mahajan, S.A. Singh, I. Sreedhar, Green hydrogen production pathways for sustainable future with net zero emissions, Fuel 359 (2024). https://doi.org/10.1016/j.fuel.2023.130131.
[18] N. Prieto, E.L. da Silva, J.R. Castiglioni, A. Cuña, Synthesis and characterization of non-noble metal cathode electrocatalysts for PEM water electrolysis, Electrochim Acta 473 (2024). https://doi.org/10.1016/j.electacta.2023.143474.
[19] J. Li, Z. Jing, H. Bai, Z. Chen, A.I. Osman, M. Farghali, D.W. Rooney, P.S. Yap, Optimizing hydrogen production by alkaline water decomposition with transition metal-based electrocatalysts, Environ Chem Lett 21 (2023). https://doi.org/10.1007/s10311-023-01616-z.
[20] T. Xiong, Z. Zhu, Y. He, M.S. Balogun, Y. Huang, Phase Evolution on the Hydrogen Adsorption Kinetics of NiFe-Based Heterogeneous Catalysts for Efficient Water Electrolysis, Small Methods 7 (2023). https://doi.org/10.1002/smtd.202201472.
[21] G. Liu, Y. Xu, T. Yang, L. Jiang, Recent advances in electrocatalysts for seawater splitting, Nano Materials Science 5 (2023). https://doi.org/10.1016/j.nanoms.2020.12.003.
[22] S. Wang, A. Lu, C.J. Zhong, Hydrogen production from water electrolysis: role of catalysts, Nano Converg 8 (2021). https://doi.org/10.1186/s40580-021-00254-x.
[23] H. Wu, C. Feng, L. Zhang, J. Zhang, D.P. Wilkinson, Non-noble Metal Electrocatalysts for the Hydrogen Evolution Reaction in Water Electrolysis, Electrochemical Energy Reviews 4 (2021). https://doi.org/10.1007/s41918-020-00086-z.
[24] H. Tüysüz, Alkaline Water Electrolysis for Green Hydrogen Production, Acc Chem Res (2023). https://doi.org/10.1021/acs.accounts.3c00709.
[25] H. Huang, C. Yu, C. Zhao, X. Han, J. Yang, Z. Liu, S. Li, M. Zhang, J. Qiu, Iron-tuned super nickel phosphide microstructures with high activity for electrochemical overall water splitting, Nano Energy 34 (2017). https://doi.org/10.1016/j.nanoen.2017.03.016.
[26] A.B. Cundy, L. Hopkinson, R.L.D. Whitby, Use of iron-based technologies in contaminated land and groundwater remediation: A review, Science of the Total Environment 400 (2008). https://doi.org/10.1016/j.scitotenv.2008.07.002.
[27] A. Casnati, M. Lanzi, G. Cera, Recent advances in asymmetric iron catalysis, Molecules 25 (2020). https://doi.org/10.3390/molecules25173889.

[28] Y. Sato, K. Sugisawa, D. Aoki, T. Yamamura, Viscosities of Fe-Ni, Fe-Co and Ni-Co binary melts, Meas Sci Technol 16 (2005). https://doi.org/10.1088/0957-0233/16/2/006.
[29] S. Anantharaj, S. Kundu, S. Noda, “The Fe Effect”: A review unveiling the critical roles of Fe in enhancing OER activity of Ni and Co based catalysts, Nano Energy 80 (2021). https://doi.org/10.1016/j.nanoen.2020.105514.
[30] T.Y. Kim, S. Jo, Y. Lee, S.H. Kang, J.W. Kim, S.C. Lee, J.C. Kim, Influence of ni on fe and co-fe based catalysts for high-calorific synthetic natural gas, Catalysts 11 (2021). https://doi.org/10.3390/catal11060697.
[31] A. Malloum, K.A. Adegoke, J.O. Ighalo, J. Conradie, C.R. Ohoro, J.F. Amaku, K.O. Oyedotun, N.W. Maxakato, K.G. Akpomie, E.S. Okeke, C. Olisah, Computational methods for adsorption study in wastewater treatment, J Mol Liq 390 (2023). https://doi.org/10.1016/j.molliq.2023.123008.
[32] H. Jung, K.-J. Noh, J. Song, H. Im, Y. Lee, H.S. Jung, S. Park, J.W. Han, Computational Screening of New Dopants for Nife-Based Layered Double Hydroxide Catalysts for Seawater Splitting, ECS Meeting Abstracts MA2022-02 (2022). https://doi.org/10.1149/ma2022-02502516mtgabs.
[33] J. Fujiki, E. Furuya, Density functional theory study of adsorption of benzothiophene and naphthalene on silica gel, Fuel 164 (2016). https://doi.org/10.1016/j.fuel.2015.10.013.
[34] S.J. Clark, M.D. Segall, C.J. Pickard, P.J. Hasnip, M.I.J. Probert, K. Refson, M.C. Payne, First principles methods using CASTEP, Zeitschrift Fur Kristallographie 220 (2005). https://doi.org/10.1524/zkri.220.5.567.65075.
[35] M.D. Segall, P.J.D. Lindan, M.J. Probert, C.J. Pickard, P.J. Hasnip, S.J. Clark, M.C. Payne, First-principles simulation: Ideas, illustrations and the CASTEP code, Journal of Physics Condensed Matter 14 (2002). https://doi.org/10.1088/0953-8984/14/11/301.
[36] P. Makkar, N.N. Ghosh, A review on the use of DFT for the prediction of the properties of nanomaterials, RSC Adv 11 (2021). https://doi.org/10.1039/d1ra04876g.
[37] B. Shan, Y. Zhao, J. Hyun, N. Kapur, J.B. Nicholas, K. Cho, Coverage-dependent CO adsorption energy from first-principles calculations, Journal of Physical Chemistry C 113 (2009). https://doi.org/10.1021/jp8094962.
[38] N.N. Tolkachev, Y.A. Pokusaeva, V.I. Bogdan, DFT Study of Potential Barriers and Trajectory of CO2 Adsorption/Desorption As Well As Dissociation on Clusters Simulating Fe (100), Fe (110), and Fe (111) Facets, Russian Journal of Physical Chemistry A 97 (2023). https://doi.org/10.1134/S0036024423080289.
[39] J.P. Perdew, K. Burke, M. Ernzerhof, Generalized gradient approximation made simple, Phys Rev Lett 77 (1996). https://doi.org/10.1103/PhysRevLett.77.3865.
[40] H.J.M. James D. Pack, Special points for Brillonln-zone integrations"—a reply, J Chem Inf Model 16 (1977).
[41] D.C. Liu, J. Nocedal, On the limited memory BFGS method for large scale optimization, Math Program 45 (1989). https://doi.org/10.1007/BF01589116.
[42] B.G. Pfrommer, M. Côté, S.G. Louie, M.L. Cohen, Relaxation of Crystals with the Quasi-Newton Method, J Comput Phys 131 (1997). https://doi.org/10.1006/jcph.1996.5612.
[43] R. Fletcher, Practical Methods of Optimization, 2000. https://doi.org/10.1002/9781118723203.
[44] M.J. Zhao, E.M. Li, N. Deng, Y. Hu, C.X. Li, B. Li, F. Li, Z.G. Guo, J.B. He, Indirect electrodeposition of a NiMo@Ni(OH)2MoOx composite catalyst for superior hydrogen production in acidic and alkaline electrolytes, Renew Energy 191 (2022). https://doi.org/10.1016/j.renene.2022.04.025.
[45] W. Wu, J. Owino, A. Al-Ostaz, L. Cai, Applying Periodic Boundary Conditions in Finite Element Analysis, Simulia Community Conference (2014).
[46] T. Wang, X.-X. Tian, Y.-W. Li, J. Wang, M. Beller, H. Jiao, Coverage-Dependent CO

Adsorption and Dissociation Mechanisms on Iron Surfaces from DFT Computations, ACS Catal 4 (2014) 1991–2005. https://doi.org/10.1021/cs500287r.
[47] D.J. Evans, B.L. Holian, The Nose-Hoover thermostat, J Chem Phys 83 (1985). https://doi.org/10.1063/1.449071.
[48] T. Lu, F. Chen, Multiwfn: A multifunctional wavefunction analyzer, J Comput Chem 33 (2012). https://doi.org/10.1002/jcc.22885.
[49] W. Humphrey, A. Dalke, K. Schulten, VMD: Visual molecular dynamics, J Mol Graph 14 (1996). https://doi.org/10.1016/0263-7855(96)00018-5.
[50] J. Park, S. Kang, J. Lee, Non-noble electrocatalysts discovered by scaling relations of Gibbs-free energies of key oxygen adsorbates in water oxidation, J Mater Chem A Mater 10 (2022). https://doi.org/10.1039/d2ta02594a.
[51] F.G.S. Oliveira, F. Bohn, A.N. Correia, I.F. Vasconcelos, P. de Lima-Neto, Fe–Co coatings electrodeposited from eutectic mixture of choline chloride-urea: Physical characterizations and evaluation as electrocatalysts for the hydrogen evolution reaction, J Alloys Compd 851 (2021). https://doi.org/10.1016/j.jallcom.2020.156330.
[52] F.G.S. Oliveira, L.P.M. Santos, R.B. da Silva, M.A. Correa, F. Bohn, A.N. Correia, L. Vieira, I.F. Vasconcelos, P. de Lima-Neto, FexNi(1-x) coatings electrodeposited from choline chloride-urea mixture: Magnetic and electrocatalytic properties for water electrolysis, Mater Chem Phys 279 (2022). https://doi.org/10.1016/j.matchemphys.2022.125738.
[53] M. Yu, E. Budiyanto, H. Tüysüz, Principles of Water Electrolysis and Recent Progress in Cobalt-, Nickel-, and Iron-Based Oxides for the Oxygen Evolution Reaction, Angewandte Chemie - International Edition 61 (2022). https://doi.org/10.1002/anie.202103824.
[54] E. Cossar, A.O. Barnett, F. Seland, E.A. Baranova, The performance of nickel and nickel-iron catalysts evaluated as anodes in anion exchange membrane water electrolysis, Catalysts 9 (2019). https://doi.org/10.3390/catal9100814.
[55] P. Błoński, A. Kiejna, Structural, electronic, and magnetic properties of bcc iron surfaces, Surf Sci 601 (2007). https://doi.org/10.1016/j.susc.2006.09.013.
[56] M.Y. Toriyama, A.M. Ganose, M. Dylla, S. Anand, J. Park, M.K. Brod, J.M. Munro, K.A. Persson, A. Jain, G.J. Snyder, How to analyse a density of states, Materials Today Electronics 1 (2022). https://doi.org/10.1016/j.mtelec.2022.100002.
[57] E.L. Silva-Ramírez, I. Cumbrera-Conde, R. Cano-Crespo, F.L. Cumbrera, Machine learning techniques for the ab initio Bravais lattice determination, Expert Syst 40 (2023). https://doi.org/10.1111/exsy.13160.
[58] J.D. Kovac, Physical Chemistry: A Molecular Approach (McQuarrie, Donald A.; Simon, John D.), J Chem Educ 75 (1998). https://doi.org/10.1021/ed075p545.
[59] L.L. Bezerra, A.N. Correia, P. de Lima-Neto, N. de K.V. Monteiro, Analysis of temperature effect in the CO2 absorption using a deep eutectic solvent: An in silico approach, J Mol Graph Model 126 (2024). https://doi.org/10.1016/j.jmgm.2023.108649.
[60] C. Lefebvre, G. Rubez, H. Khartabil, J.C. Boisson, J. Contreras-García, E. Hénon, Accurately extracting the signature of intermolecular interactions present in the NCI plot of the reduced density gradient: Versus electron density, Physical Chemistry Chemical Physics 19 (2017). https://doi.org/10.1039/c7cp02110k.

SUPPLEMENTARY MATERIAL

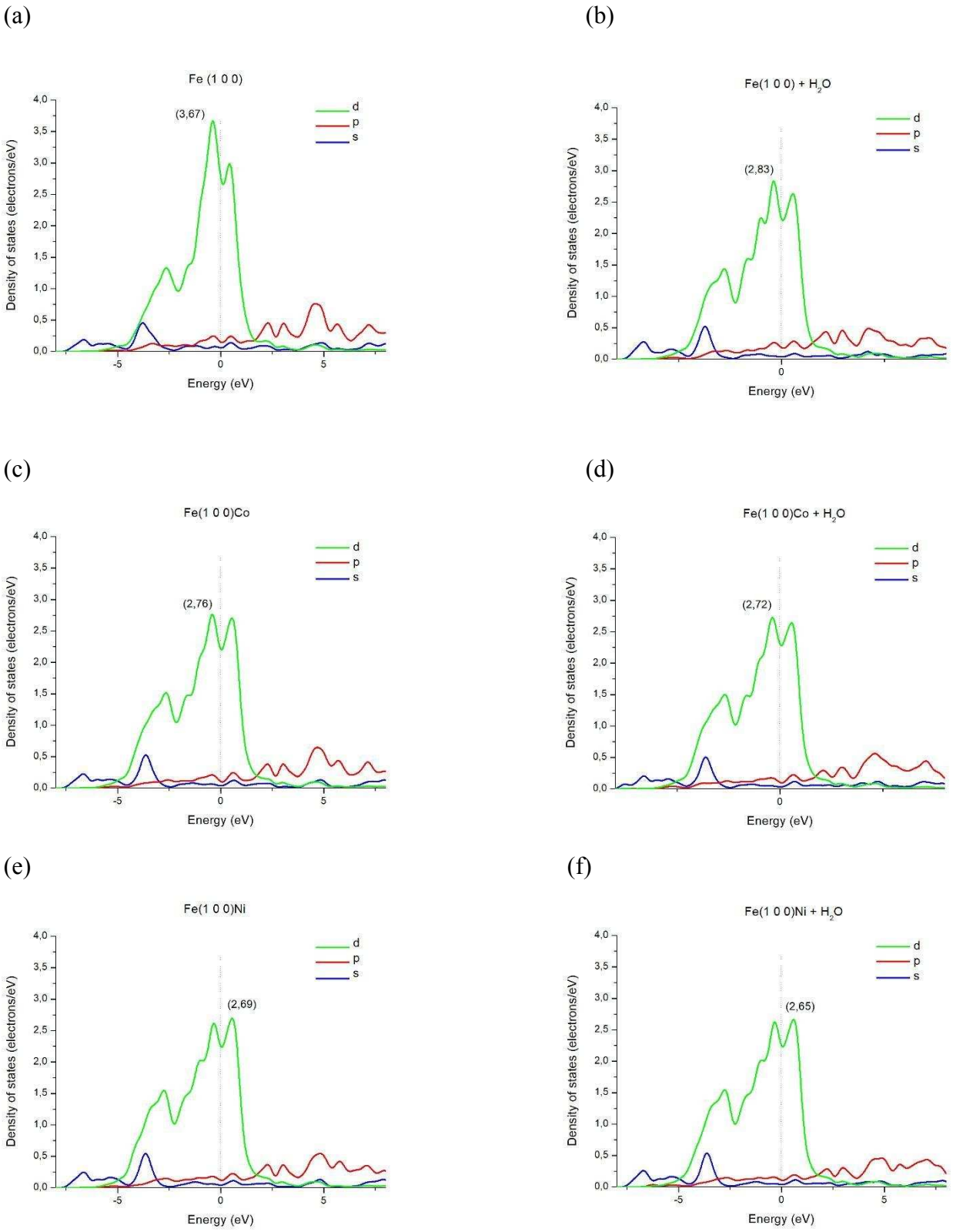

Fig. S1. PDOS for a) Fe(1 0 0) surface, c) Fe(1 0 0)Co alloy and e) Fe(1 0 0)Ni alloy without water and for b) Fe(1 0 0) surface, d) Fe(1 0 0)Co alloy and f) Fe(1 0 0)Ni alloy with water.

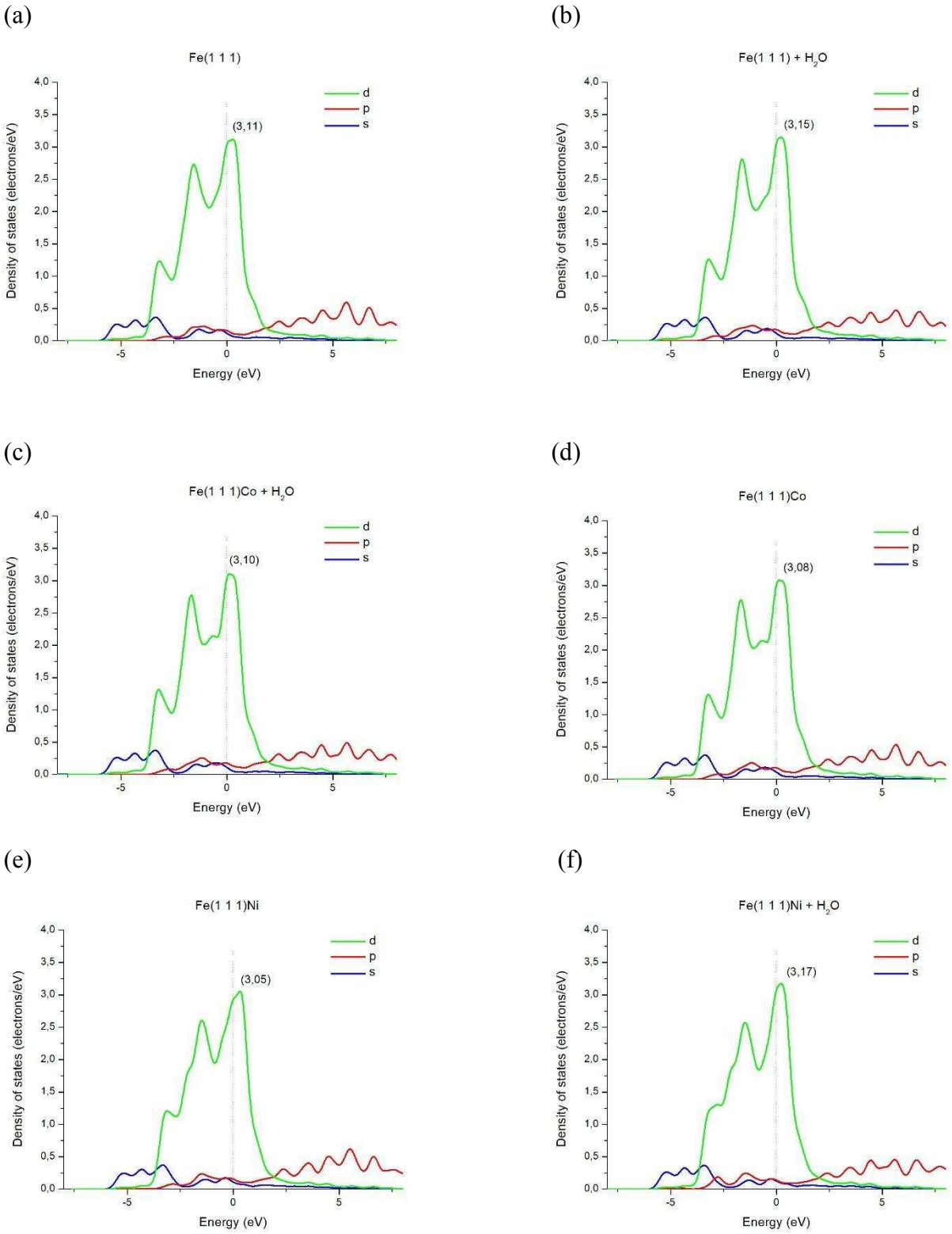

Fig. S2. PDOS for a) Fe(1 1 1) surface, c) Fe(1 1 1)Co alloy and e) Fe(1 1 1)Ni alloy without water and for b) Fe(1 1 1) surface, d) Fe(1 1 1)Co alloy and f) Fe(1 1 1)Ni alloy with water.

(a)

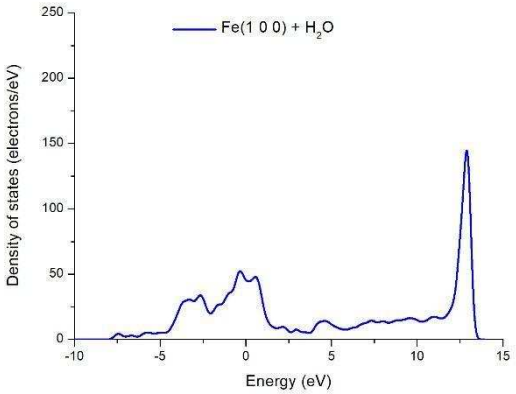

(b)

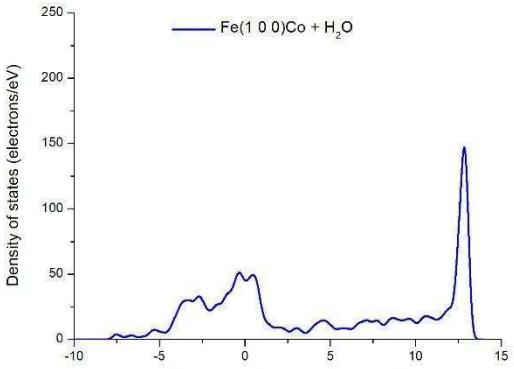

(c)

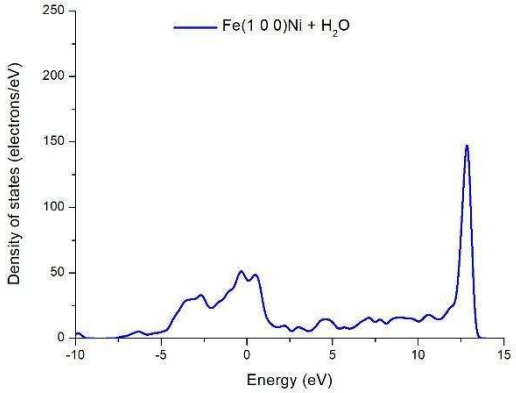

Fig. S3. TDOS for a) Fe(1 0 0) surface, c) Fe(1 0 0)Co alloy and e) Fe(1 0 0)Ni alloy with water.

(a)

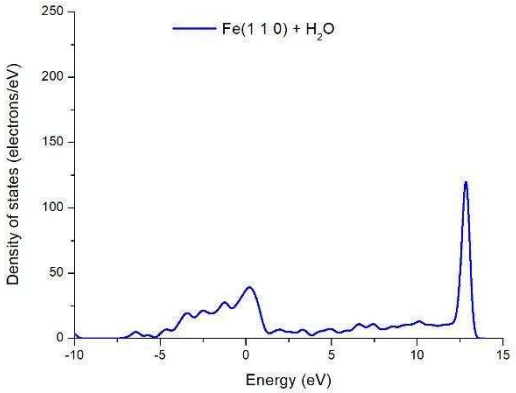

(b)

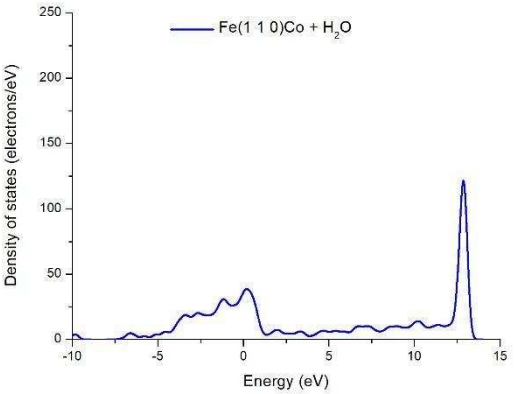

(c)

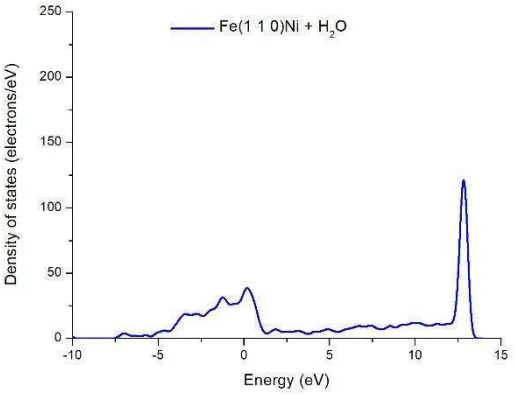

Fig. S4. TDOS for a) Fe(1 1 0) surface, c) Fe(1 1 0)Co alloy and e) Fe(1 1 0)Ni alloy with water.

(a)

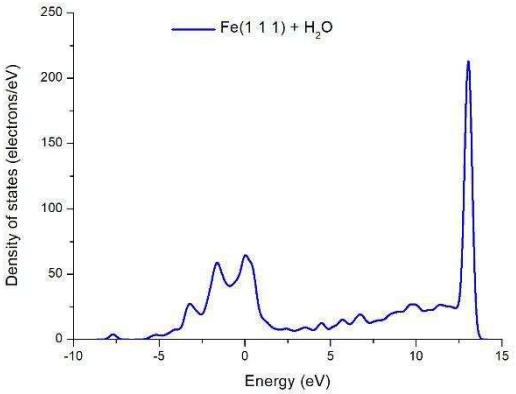

(b)

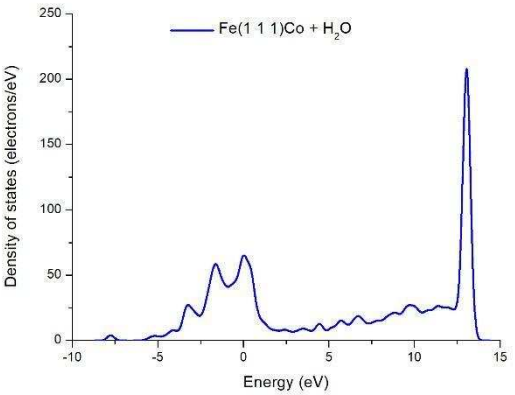

(c)

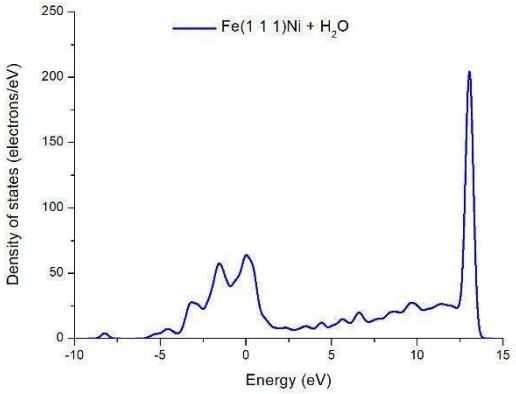

Fig S5. TDOS for a) Fe(1 1 1) surface, c) Fe(1 1 1)Co alloy and e) Fe(1 1 1)Ni alloy with water.

3 CONCLUSION

Simulations performed using DFT determined the Gibbs energy of adsorption and density of states for all analyzed systems. This analysis revealed that the most stable symmetry cut for working with iron and its metallic alloys is (1 1 0), followed by (1 0 0). The stability of the symmetry cuts is directly related to the surface size, i.e., the spatial arrangement of atoms in the crystal lattice, which reduces lateral repulsions and favors adsorbate adsorption at active sites. During the adsorption study, it was observed that the water molecule approaches the surface preferentially with the oxygen atom pointing toward it, due to the donation and acceptance of electronic states between iron and the adsorbate's oxygen. It was also determined that the lowest-energy site for water adsorption can vary with the Miller index. From the PDOS for the (1 1 0) symmetry cut, the addition of cobalt and nickel increased the density of states of the iron atom on the surface. This demonstrates that interaction with the adsorbate occurs preferentially at iron atoms because they have a higher density of states available for interaction.

A consistent trend was observed wherein the partial density of states of iron always decreases with water adsorption across all Miller indices. This occurs due to the antibonding orbitals in the water molecule, causing iron to donate density of states during adsorption. Based on all the data obtained in this work, it can be concluded that the first adsorption step, for the water molecule on pure iron surfaces and their Fe-Co and Fe-Ni alloys occurs spontaneously, given the negative values of Gibbs energy of adsorption. However, the focus of this study was to analyze the adsorption of water in the materials investigated, and it can be concluded that the methodology employed successfully enabled the verification of the adsorption stage in the iron alloys.

From a future work perspective, it is also possible to verify the chemical kinetics of this reaction for each of the systems to determine which alloy has the best catalytic activity for the production of green hydrogen. Furthermore, it is also possible to analyze which stage is decisive for the reaction.

REFERENCES

ALOBAID, Aisha; WANG, Chunsheng; ADOMAITIS, Raymond A. Mechanism and Kinetics of HER and OER on NiFe LDH Films in an Alkaline Electrolyte. **Journal of The Electrochemical Society**, Pennington, NJ, v. 165, n. 15, 2018.

ANWAR, Shams *et al.* Recent development in electrocatalysts for hydrogen production through water electrolysis. **International Journal of Hydrogen Energy**, Oxford: Elsevier, v. 46, n. 63, 2021.

ASHCROFT, Neil W.; MERMIN, N. David. Solid state physics (holt, rinehart and winston, new york, 1976). There is no corresponding record for this reference, 2005.

BLAKELY, D. W.; SOMORJAI, G. A. The stability and structure of high miller index platinum crystal surfaces in vacuum and in the presence of adsorbed carbon and oxygen. **Surface Science**, Amsterdam, v. 65, n. 2, 1977.

BŁOŃSKI, P.; KIEJNA, A. Structural, electronic, and magnetic properties of bcc iron surfaces. **Surface Science**, Amsterdam, v. 601, n. 1, 2007.

CASNATI, Alessandra; LANZI, Matteo; CERA, Gianpiero. Recent advances in asymmetric iron catalysis. Molecules, 2020.

CHANG, Jiuli *et al.* Nickel iron alloy embedded, nitrogen doped porous carbon catalyst for efficient water electrolysis. **Applied Catalysis A: General**, Amsterdam, v. 650, 2023.

CUNDY, Andrew B.; HOPKINSON, Laurence; WHITBY, Raymond L. D. Use of iron-based technologies in contaminated land and groundwater remediation: A review. **Science of the Total Environment**, Amsterdam: Elsevier, v. 400, n. 1–3, 2008.

GRÜNERT, Wolfgang; KLEIST, Wolfgang; MUHLER, Martin. **Catalysis at surfaces.** *[S.l.: S.n.]*.

HOFFMANN, Roald. How Chemistry and Physics Meet in the Solid State. **Angewandte Chemie International Edition in English**, Weinheim, v. 26, n. 9, 1987.

HUANG, H. M.; LUO, S. J.; YAO, K. L. First-principles study of the stability and the electronic structure of NiO/MgO interface. **Computational Materials Science**, Elsevier v. 50, n. 1, 2010.

HUANG, Huawei *et al.* Iron-tuned super nickel phosphide microstructures with high activity for electrochemical overall water splitting. **Nano Energy**, [*s. l.*], v. 34, 2017.

KHAN, Muhammad Arif *et al.* Recent Progresses in Electrocatalysts for Water Electrolysis. **Electrochemical Energy Reviews**, [*s. l.*], 2018.

KWAWU, Caroline R. *et al.* CO2 activation and dissociation on the low miller index surfaces of pure and Ni-coated iron metal: A DFT study. **Physical Chemistry Chemical Physics**, Cambridge, v. 19, n. 29, 2017.

LADD, Mark. Miller Indices. ***In*: Bonding, Structure and Solid-State Chemistry**, *[s.l.: s.n.]*.

PALERMO, S. A. *et al.* Nature-based solutions for urban stormwater management: An overview. *In*: 2023.

SAHA, Priyanka *et al.* Grey, blue, and green hydrogen: A comprehensive review of production methods and prospects for zero-emission energy. **International Journal of Green Energy**, Philadelphia, 2024.

SEBBAHI, Seddiq *et al.* Assessment of the three most developed water electrolysis technologies: Alkaline Water Electrolysis, Proton Exchange Membrane and Solid-Oxide Electrolysis. **Materials Today: Proceedings**, [*s. l.*], v. 66, 2022.

SILVA-RAMÍREZ, Esther Lydia *et al.* Machine learning techniques for the ab initio Bravais lattice determination. Expert Systems, [*s. l.*], v. 40, n. 2, 2023.

SINGH, Udayan; BANERJEE, Sudhanya; HAWKINS, Troy R. Implications of CO2 Sourcing on the Life-Cycle Greenhouse Gas Emissions and Costs of Algae Biofuels. **ACS Sustainable Chemistry and Engineering**, Washington, v. 11, n. 39, 2023.

SKOGH, Mårten *et al.* The electron density: a fidelity witness for quantum computation. **Chemical Science**, [*s. l.*], v. 15, n. 6, 2023.

TANG, Dan *et al.* State-of-the-art hydrogen generation techniques and storage methods: A critical review. **Journal of Energy Storage**, Elsevier, 2023.

TÜYSÜZ, Harun. Alkaline Water Electrolysis for Green Hydrogen Production. **Accounts of Chemical Research**, Washington, 2023.

WANG, Shan; LU, Aolin; ZHONG, Chuan Jian. Hydrogen production from water electrolysis: role of catalysts. **Nano Convergence**, [*s. l.*], 2021.

WU, Huimin *et al.* Non-noble Metal Electrocatalysts for the Hydrogen Evolution Reaction in Water Electrolysis. **Electrochemical Energy Reviews**, Heidelberg: Springer, 2021.

ZENG, Kai; ZHANG, Dongke. Recent progress in alkaline water electrolysis for hydrogen production and applications. **Progress in Energy and Combustion Science**, Oxford, 2010.

ZENG, Shu Pei *et al.* Lamella-heterostructured nanoporous bimetallic iron-cobalt alloy/oxyhydroxide and cerium oxynitride electrodes as stable catalysts for oxygen evolution. **Nature Communications**, London, v. 14, n. 1, 2023.

APPENDIX A – PAPER PUBLISHED

Journal of Molecular Liquids 433 (2025) 127973

Contents lists available at ScienceDirect

Journal of Molecular Liquids

journal homepage: www.elsevier.com/locate/molliq

Computational study of water adsorption on iron surfaces and metallic alloys

Gizele N. Castro, Lucas L. Bezerra, Leonardo P. da Silva, Pedro de Lima Neto, Adriana N. Correia, Norberto K.V. Monteiro *

Departamento de Química Analítica e Físico-Química, Centro de Ciências, Universidade Federal do Ceará, Campus do Pici, Bloco 940, 60440-900 Fortaleza, CE, Brazil

ARTICLE INFO

Keywords:
Green hydrogen
Iron alloys
Adsorption
DFT

ABSTRACT

One solution to reduce the concentration of greenhouse gases (GHG) in the atmosphere is to replace fossil fuels with clean and renewable energy sources, such as green hydrogen. However, the method used, water electrolysis, is not yet widely used in the market due to its high cost since this process uses electrocatalysts based on noble metals, scarce in nature, such as iridium and platinum. The present study uses a computational approach to investigate the water adsorption stage in iron, iron-cobalt and iron-nickel alloys; geometric optimization, molecular dynamics and electronic properties calculations were performed based on Density Functional Theory (DFT). The computational results show that the Gibbs energy of water adsorption is more spontaneous in the following order of symmetry cuts: (1 1 0) > (1 0 0) > (1 1 1). The addition of a nickel atom to the metal surface increased the partial density of states of the adjacent iron atoms, facilitating the adsorption of the water molecule since it was in the position between the iron atom and the nickel atom that a greater availability of electronic states for the interaction was observed. In addition, the adsorption of the water molecule on the metal surface decreased the partial density of states of the iron atom. This behavior was observed for pure iron and metal alloys when water interacts with the most favorable active site on the surface, indicating that the iron atom donates the density of states to the water molecule for adsorption.

1. Introduction

It is estimated that 2030 energy demand will increase by up to 50 %, according to the International Energy Agency (IEA) [1], because the world's population is growing rapidly, and the search for energy is becoming increasingly necessary [2]. However, it is known that since the Industrial Revolution, the most used energy source worldwide has been fossil fuels, such as oil and natural gas [3]. Although it is responsible for 95 % of energy supply, fossil fuel specifically has, among others, an increased concentration of gases such as carbon dioxide (CO_2) and methane (CH_4) in the atmosphere, which contributes to global warming. The increase in the planet's temperature causes climate change accompanied by environmental disasters.

Therefore, in 1997, the Kyoto Protocol was adopted to considerably reduce the emission of greenhouse gases (GHG) [4] into the atmosphere. Furthermore, the amount of this raw material on the planet is limited and rapidly depleting, which makes fossil fuels non-renewable energy sources. Therefore, searching for renewable energy sources with low or no GHG emissions is essential, and Green hydrogen stands out among the alternatives [5].

To be considered green, hydrogen gas must be produced using methods considered green, and for this, the process must be free of GHG emissions. However, around 95 % of this gas produced worldwide comes from non-renewable sources, such as natural gas [6]. Under these circumstances, a clean and effective way to produce hydrogen gas is through water electrolysis [7] with electrical energy responsible for initiating the electrochemical reactions of the process coming from renewable and clean sources such as wind and solar energy [8,9].

Electrolysis consists of an electrocatalytic decomposition, requiring a cathode and an anode responsible for the electrochemical half-reactions. These electrodes are connected to an external energy source, thus forming a conductive circuit where electrons can be transferred [10]. To break the water molecule and develop hydrogen gas, the water molecule first approaches the electrode in specific locations on the surface. The water molecule will be adsorbed in the site with the lowest energy barrier, which can favor the reaction. Some mechanisms, widely studied

* Corresponding author.
E-mail address: norbertokv@ufc.br (N.K.V. Monteiro).

https://doi.org/10.1016/j.molliq.2025.127973
Received 10 March 2025; Received in revised form 5 June 2025; Accepted 13 June 2025
Available online 13 June 2025